15th International Symposium on Particle Image Velocimetry – ISPIV 2023
June 19–21, 2023, San Diego, California, USA

Concentration measurements in the near-field of a transient jet using planar Mie scattering

Benjamin A. K. Hartz[1], Knud Erik Meyer[1]*

[1] Technical University of Denmark, Dept. of Civil and Mechanical Engineering, Kgs. Lyngby, Denmark

* keme@dtu.dk

Abstract

Results from a near-field transient jet shooting into a quiescent medium based on concentration measurements using planar Mie scattering and a high-resolution high speed camera are presented. Data are analysed to show the challenges as signal trapping, precision due to signal-to-noise ratio and the usability by comparing the data to findings from literature. The presented data are produced using a free jet under no-slip condition at a Re ≈ 62.000, 25 ms after valve opening up to 22 nozzle diameters into the domain.

Introduction

To support a lower carbon footprint from transport of goods by ship, large two-stroke diesel engines are being adapted for new types of fuel like methane and ammonia. To avoid the expensive compression to the very high pressures used in traditional fuel nozzles, a new solution is to inject the fuel in gaseous form into the engine cylinder in a way that allows for premixing before ignition. It is challenging to achieve sufficient mixing within the short time available before ignition.

Investigation of the concentration and velocity in the free jet near-field have been done in several studies, (Pitts (1991a,b), Birch et al. (1978)) but in common is that it is only at a fairly low Reynolds numbers span from around 3.000 till 70.000. For the higher Reynolds number studies, most look at velocities, Mach disk location and penetration (e.g. Hill and Ouellette (1999)), while one study used planar Mie scattering to visualize a supersonic jet for Mach disc investigation (Karthick et al. (2016)). Jets at ”no-slip” conditions (jet nozzle flushed with wall) are not commonly investigated. Romano (2002) investigated the difference between ”no-slip” and ”free-slip” (free jet) condition using Laser Induced Fluorescence (LIF) in close near field, while Verzicco and Orlandi (1995) used numerical methods to quantify the starting vorticies. Therefore, the present study is set along to investigate the mixing in near-field no-slip conditions using planar Mie scattering for concentration measurements and evaluate different designs of nozzles and injection strategies.

Laser Induced Fluorescence (LIF) is popular for concentration measurements (Dahm and Dimotakis (1987, 1990), Romano (2002)), along with Rayleigh Light Scattering (RLS) (Pitts (1991a,b)) and to some extend Raman Spectroscopy (Birch et al. (1978)).

The planar Mie scattering concentration method used in this study is not as widely used, but Rosensweig (1959) developed a technique called the ”sol-scattering light technique”, further explained in Rosensweig et al. (1961). Becker (1961) used the technique in his thesis and several following studies (Becker et al. (1967c,b,a); Becker and Massaro (1968)). The ”sol-technique” contains of a point focused light source, where a lens and slit focus the light a into phototube. In other studies they refereed to this technique as ”smoke scattering” and ”nephelometry” (Dowling and Dimotakis (1990); Pitts (1991a)). Here nephelometry is a more common method used in pharmaceutical laboratories, along with turbidimetry, for determining concentrations in e.g. mixed particle solutions since the 1970s. For the ”sol-scattering” used by Becker (1961), it was described that the beam diameter used to determined the concentration fluctuations was found to be satisfactory at 1/12 in (approx. 2.12 mm), which makes it comparable to imaging into a single pixel on a camera sensor.

Further Long et al. (1979) changed the light source and used a laser for planar concentration measurements using camera to get estimations in a jet near field. Here some have worked towards combining concentration and velocity estimations based on the same images. (Simoens and Ayrault (1996); Ingvorsen et al. (2011))

Experimental setup

To accommodate the demand of later experiments, a transient jet system that allow for use of different nozzle designs with exit diameters up to 20 mm was built. The system can reach chocked underexpanded conditions. Further, the design makes it possible to introduced pre-jet treatment for the flow to investigate more than just nozzle geometries on the affect of the mixing probabilities. For the experiments here the nozzle diameter used is 13.3 mm. Figure 1 shows the experimental setup. With the setup it is theoretically possible to reach Reynolds numbers between 30.000 to 1.000.000, dependent on the nozzle size mounted and back-pressure setting. With a small setup modification free-slip wall conditions is achievable.

The jet is connected to a 50 L pressure tank that handles pressures up to 10 bar. To monitor the tank pressure a GEMS 0-10 bar pressure transducer (3100B0010G01B000) is used. As it was not possible to find a fast acting valve large enough for a single line, four pressure lines of Ø13 mm inner diameter connect the tank and jet. Mounted on each line there is a filter (Norgreen coalsing 0.01 µm F84C-4GD-QP0) and fast acting solenoid valve (Bürkert, Ø12 orifice, 6240-A12,0FFVAGM84-K-024/DC-16*NA38). As the orifice opening of the valve is only Ø12, this limit the nozzle sizes possible. With the four lines it provide a the surface area ratio between the feeding system and the largest nozzle at $A_{valve}/A_{20,nozzle} = 1.44$. As the system has to be characterized by hotwire, the filters are added to remove the small particles in the system so the hotwire is not damaged at choked conditions.

To control the setup, a Nation Instrument (NI) CompactRIO (9068) is used with in-house written code. All critical timing is done on the Field Programmable Gate Array (FPGA) for signalling the valves and camera (Photron NOVA S9 with a 50mm Nikkor F/1.4 lens set to 10.000 fps with 512x1024 image resolution). The 50mm lens gives a resolution of 0.30 mm/pixel, while some test are done with a 60mm lens providing 0.26 mm/pixel.

The camera is synchronized with an Innolas Nanio Nd:YAG 532-18-Y pulsed laser through the built-in synchronization module. Sampling of the pressure is done on a NI 9215 analog sampling module with a usable precision of 19.1 Pa/bit. Further an automated program is coded to reduce the chance of errors in the data acquisition. To conduct the experiments there had to be designed a setup that made it possible to contain the jet and particles, while keeping it unaffected by unwanted wall effects. Here George (1990) described two constraints; one on the co-flow and one for the screen effect on a flow. (see eq. (1))

$$U_0 H < U\delta \quad \& \quad \frac{1}{2} C_p V_s^2 \ll \overline{v^2} \tag{1}$$

Here $U_0 H$ can be seen as a representation of the co-flowing volume, while $U\delta$ is the volume flow in the jet. The criteria describe that the volume in the co-flow has to be less than that of the jet. The second part tell that the entertainment velocity energy, $\frac{1}{2} C_p V_s^2$, has to be at least *two* orders of magnitudes less than the r.m.s. of the fluctuating velocity part in the radial direction to the centerline $\overline{v^2}$. Based on the choice of screen and pressure coefficient at the Reynolds number for the entertainment velocity, then it is possible to determined if the jet will develop under free conditions or under box constraints.

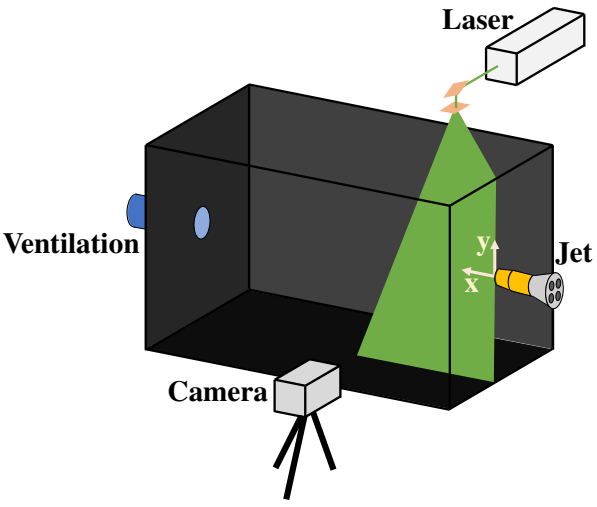

Figure 1: Sketch of the experimental setup

By utilizing the work by George (1990) the box size was calculated using the largest nozzle settings possible with a mass-flow corresponding to a stagnation (P_0) to environment pressure (P_{env}) difference of $P_0/P_{env} = 3$, for the 20 mm nozzle size (D_{20mm}) and an unaffected jet $30D_{20mm}$ into the box. This lead to construction of a box that is symmetrical in height and width of $30D_{20mm}$ and $70D_{20mm}$ long. The material chosen for the box is cast 8 mm thick acrylic plates with a claimed 93% light transmissibility. A sketch of the setup is seen in figure 1.

The jet system is at the moment only calibrated for known exit velocities up to 140 m/s due to hotwire system limitations at current state. This makes it possible to reach Reynolds numbers of approximately 120.000 for the 13.3 mm nozzle.

Definition of Mixing

One question to answer before evaluating results is how to define mixing in the jets concentration field with several existing statistical methods. Hawthorne et al. (1948) worked with mixing and combustion in turbulent jets and defined a scalar called "unmixedness factor", which is the r.m.s. of the fluctuating value of concentration in points over a time period ($C' = C_k - \overline{C}$, where C_k is the instantaneous concentration and $\overline{C}$ is the time-mean concentration). It was shown evaluated against the reciprocal time-mean concentration value ($1/\overline{C}$). This has further evolved into the expression:

$$\phi_{unmix} = \frac{\sqrt{\overline{C'^2}}}{\overline{C}} \tag{2}$$

Which is used in several studies for evaluating mixing of jets. (e.g. Pitts (1991a,b); Birch et al. (1978); Dahm and Dimotakis (1990))

60 years later Kukukova et al. (2009) worked with analysing mixing for chemical processes using cameras. The study evaluate on how to define mixing between two fluids and which different approaches could be used. From an extensive analysis different methods were discussed and a new definition called "coefficient of variance (CoV)" was shown as:

$$\phi_{CoV} = \sqrt{\frac{1}{N_t}\sum_{i=1}^{N_t}\left(\frac{C_i - C_{mean}}{C_{mean}}\right)^2} \tag{3}$$

Where N_t is the number of pixels, C_i is the concentration seen in a pixel and C_{mean} is the average concentration over an image.
The definition of CoV and unmixedness is very similar, but differ in one main aspect. CoV is defined for an area of interest at a frozen time while the unmixedness is for a point in time. Kukukova et al. (2009) described that the CoV was not alone enough to quantify if two fluids were well mixed within an area of investigation, illustrated by a simple 16x16 checkerboard example with 12 different fluid problems. Here it was shown that identical CoV values could have very visual different results and therefore more information is needed to evaluate how well two fluids are mixed. To provide an evaluation method for mixing, Kukukova et al. (2009) used the work of Massey and Denton (1988) and reworded the five proposed dimensions for evaluate mixing for a broader range of problems. Short description of the five dimensions are given below in the context of the present study

Evenness is the uniformity of concentration in the fluid.

Clustering is the degree of spatial continuity or adjacency of minor structures in the injected fluid.

Exposure determines the rate of reduction in segregation between the fluids.

Density is a measure used for expressing the population density as a variable. In most fluid mixing problems it is seen as a global constant.

Centralization can be described as parts with high density of unmixed fluid that tend to concentrate around certain areas, which is to clustering for fluid problems.

When working with tracking particles in fluids, centralization could be used as a parameter expressing particle clouds, but for pure fluid mixing, without resuluting particles, its evaluation is similar to clustering and is not as applicable. Density is a parameter expressed in mass per volume and for multiphase flows it may vary substantially over a mixing area. But for this study it will not be used. Exposure show promise during longer time dissipation mixing in solutions, as it quantify the contact between fluids and the rate of reduction in separation. As this study analyse high Reynolds number flow, the effect of dissipation, in regards of fluid mixing, has a low effect and will not be considered. For evaluation of mixing for a transient jet, the unmixedness (and CoV) can be used as an indication of the evenness, as it describe the concentration fluctuations in respect to the mean. Clustering/structure detection is not as easy to perform for the current problem. Here it is proposed to use Proper Orthogonal Decomposition (POD) in order to analyse the dominant structures and their influence on mixing.

Over the years several, POD methods has been developed as the original POD (Lumley (1967)), snapshot POD (Sirovich (1987)) and several other methods, where several of the methods have been demonstrated for turbulent flows (Sieber et al. (2016); Hilberg and Fiedler (1994); Lam (2013)). POD is most commonly applied on turbulent stationary problems, where large data series in time are used to get uncorrelated time data. For a transient jet a different approach is necessary. The experiment is repeated to get uncorrelated shots with identical starting conditions. This will provide snapshots at different time-steps that can be used for analysing jet behavior. It is further a complication that the jet only partly covering the image frame, which will greatly affect the value of ϕ_{CoV} as a great number of pixels are unused. (See figure 4 for examples of snapshots of shots)

With respect to the above, it is decided to use the unmixedness formulation (ϕ_{unmix}) by Hawthorne et al. (1948) for evaluation of the evenness, compared with centerline point measurements from litterature. To evaluate clustering along with evaluation on the mixing mechanism, the snapshot POD is suggested, but will not be part of the present work.

Experimental Methodology

Particle flow

The concentration is traced with particles (droplets) from a Laskin nozzle particle generator using glycerol as liquid. Particle sizes are $D_p = 0.71 \pm 0.52\ \mu m$ measured with a TSI aerodynamic particle sizer 3321 APS model 33. As high velocity flows are expected, a check on the particles flow tracking is necessary. Using the particle size the Stokes number for 95% of the particles is calculated.

$$\mathrm{Re}_{p,95} = \frac{D_{p,95}\rho_p U_{jet,max}}{\mu_{air}} = 26.486\,[-] \qquad S_{p,95} = \mathrm{Re}\frac{D_{p,95}}{18D_L} = 0.14\,[-] \tag{4}$$

Here $S_{p,95}$ is the upper 95% confidence interval Stokes number, $\mathrm{Re}_{p,95}$ is the upper 95% confidence interval Reynolds number for the particles, $D_{p,95}$ is the maximum particle size within the 95% confidence interval from the particle generator, ρ_p is the particle density, $U_{jet,max}$ is the maximum velocity reachable for the jet (here 313 m/s is used), μ_{air} is the air dynamic viscosity and D_L is a characteristic length (here the 13.3 mm nozzle diameter) (Raffel et al. (2018)).

The calculated Stokes number is close to $S_{95max} < 0.1$ which means around 95% of the particles follow the flow for all jet velocities into the sonic range, with a tracing accuracy around 1%. But the average particle size have a Stokes number of $S_{avg} = 0.045$ [-] which is $S_{avg} \ll 1$ and most particles will follow the flow with better tracing accuracy than the 1% (Tropea et al. (2007)).

Calibration

To quantify the concentration of the jet, the light intensity has to be correlated to concentration. Becker (1977) showed that under an assumption of constant particle size distribution, light scattered from an illuminated area is proportional to the number density of the particles. Preliminary studies by Eberhard and Munck (2020); Massalkhi and Iqbal (2022) used a similar setup as shown in figure 1 for jet shots in the range of Re = 20.000. Both showed that the concentration response with the particle concentration is linear and only a two-point calibration was needed, by taking images with no seeding and use the seeded images before jet shots as second point. Both studies saw some discrepancy from the expected concentration. The discrepancy from the expected concentration comes down to factors introduced by the system setup and method that influence measurements results including main issues as: Gaussian shaped beam profile from the Nd:YAG laser, window visibility, reflections, background illumination, light extinction, signal trapping and marker shot noise (Ingvorsen et al. (2011)).

In attempt to mitigate background illumination, reflections and contain the laser for safety, the setup is placed inside a test chamber, which also works as a darkroom removing light and reflections from surroundings. Further, the floor and back-wall of the containment box is coated with Black 3.0 paint by Stuart Semple (similar to ventablack), which have shown good results. A line of laser light is still visible on the wall with the jet entrance (see e.g. figure 2b or figure 4). Further, the window visibility is not an issue for this setup, as the laser sheet is perpendicular through the top plate, while the camera is placed parallel to the window (see figure 1).

Accounting for the beam profile and the light extinction is done by a two-point calibration for every pixel at each shot. The calibration is based on the assumption of a linear relationship for the light response

on particle concentration as shown in the preliminary studies and results from Becker (1977). To make the two-point calibration, a series of images are taken at no seeding used as the point indicating 100% jet fluid concentration (1.0), while images taken just before the valves are opened for a shot represent 0% jet fluid concentration (0.0). Evaluation of the precision for the linear assumption will need more data than present and be part of further studies, but results later will show this is a fair assumption.

Signal trapping happens when light attenuate from the particles filling the space between the jet and window. To check the effect of this on the estimated visible concentration measurements, the seeding amount were varied while keeping camera and laser intensity parameters constant. Results of this are seen in figure 2a. With lower particle concentrations the trapping effect decrease, but with a lower light response if the camera and laser settings are kept constant. However, along with the decreased trapping effect, the marker shot noise increase with a lower average grayscale value and fluctuations from pixel to pixel concentrations increase. It suggest that more light and less seeding is the optimal choice, but preliminary tests have shown that more light and less particles, while keeping the average grayscale value, do not mitigate the signal trapping. The increased light intensity result in an increased scattering that then reduce the benefits due to the low efficiency for observing Mie scattering at the 90° viewing angle. Another possibility to decrease the trapping effect is to reduce the particle filled area between the jet and camera. Further, the confidence interval is highly affected by the zone from $0D_{nozzle}$ till $0.4D_{nozzle}$ with a low visible concentration, which is most profound for the low average grayscale values. Though this zone of low visible concentration might be an effect of light reflection. As the nozzle is made of brass, it produce a glare from the laser sheet, when the nozzle inside is hit, a larger grayscale response is seen near the jet entrance. This increase in grayscale value, with respect to the results in figure 2a, can explain the concentration drop seen. An issue further arose with the camera at low grayscale values, as distinct sensor artifacts got visible near the jet core (see the vertical lines in the concentration field in figure 4a close to the jet entrance).

Sample size estimation

Determining the sample size to achieve statistical good results is found based on a variability analysis of a test dataset. To calculate the estimation precision the following expressions were used:

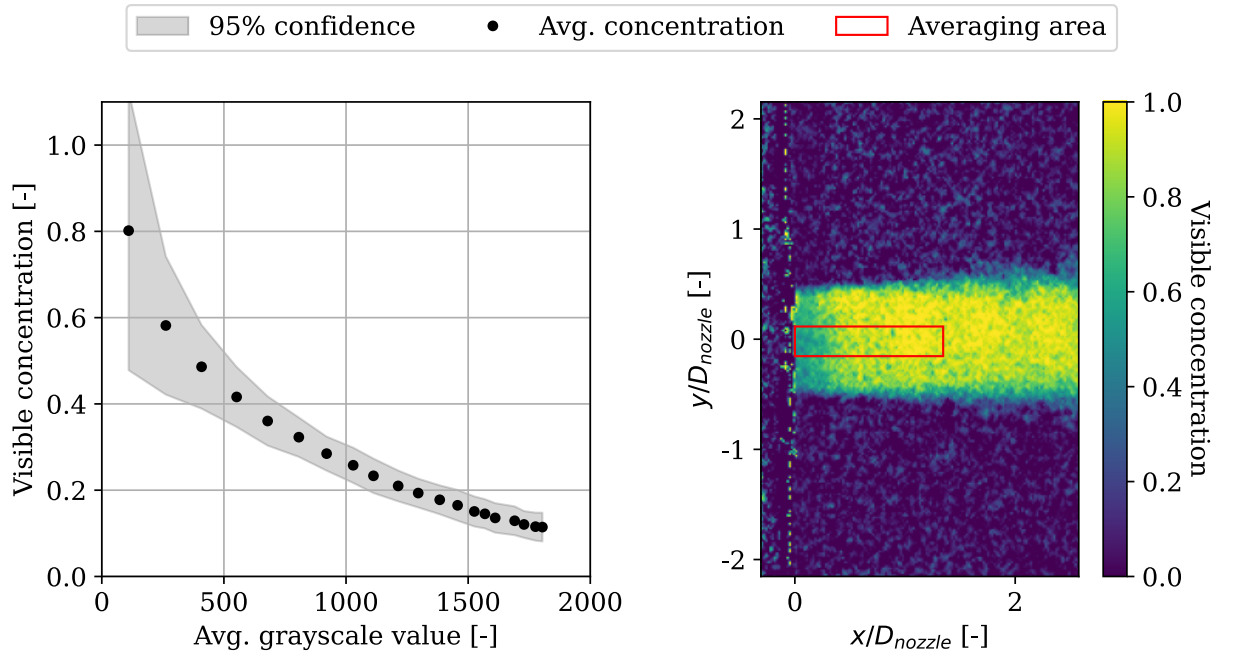

Figure 2: (a) is the visible concentration after conversion shown against the average grayscale value seen on the raw image by the camera sensor at 25 ms after the valves are opened for jet snapshots. (b) is the example image showing where the binned averaging area is chosen in the jet.

$$\varepsilon_{mean} = \frac{1}{\sqrt{N}} \frac{C_\sigma}{\overline{C}} \qquad \varepsilon_{var} = \frac{1}{\sqrt{N}} \frac{C_{\sigma^4} - C_{\sigma^2}}{C_{\sigma^2}} \tag{5}$$

Where ε_{mean} is the averages' relative statistical error and ε_{var} is the variances', N is the number of samples, C_σ is the concentration standard deviation, C_{σ^2} is the concentration variance and C_{σ^4} is the concentrations 4^{th} moment around the mean.

By using the expressions in (5) on a dataset of 200 samples with an average grayscale value of 1500, the plots in figure 3 were made showing the relative statistical error per pixel based at a snapshot 25 ms into a jet shot. A clear indication of the shot is visible with a low error, while the surrounding fluid, where there should be zero concentration, show a larger error. As only noise influence the estimate of $\overline{C}$ and C_σ in these areas, the $\overline{C}$ is a small value increasing the influence of C_σ resulting in a high error estimator in fluid surrounding the jet. Choosing a sample size of 200 provide well estimated mean values over most of the data as see in figure 3a. Around the core from the wall until $5D_{nozzle}$, the estimated mean deviate less than 1% from the "true mean". From $5D_{nozzle}$ and till the end of the visible range the error is below 5%. The background show an average error of 5 till 9%. Near the edges in the shear layer of the jet, it fades towards the background error. By comparing with the shear layer with high variability seen in figure 3b, the same structures are visible with small areas at higher error in figure 3a. This suggest that the mean lack precision if high detailing of these areas are of interest.

In figure 3 there is further seen a decrease in the background error below, and a small amount just above, the jet, most distinct near the jet entrance. This decrease in the background error could be a results of signal trapping and light scattering. As particles are moved by the jet, the laser sheet will have some free passage and the reduction in scattering could reduce the fluctuations that produce the background noise.

Further the error of the variance follow the same trend as the mean, but with a background noise value 10 to 15%. Around the jet core from the wall until $3D_{nozzle}$ the variance error is indistinguishable from the background error. From $3D_{nozzle}$ till $20D_{nozzle}$, between shear layers, there are some structures that are distinguishable from the random error. 18-$20D_{nozzle}$ till the end of visible range it again fall back towards the background error values, which could indicate that the signal response fade due to low light or signal trapping, or including more samples could provide more information for this zone. In the shear layers there are clusters with errors above the 20% suggest the need for more samples if the shear layer is of interest.

Based on the results from figure 3, 200 samples are found sufficient for the use in the test conducted for this proceeding as the mixing will be compared to literature results along the centerline of the jet, which is well resolved. The dataset at lowest sensor response presented later, only contain 100 samples and the same analysis show that the mean error for the centerline is below 4% for the whole visible range, while the variance fluctuate around 14% to 17% with a background noise around 18% to 35%.

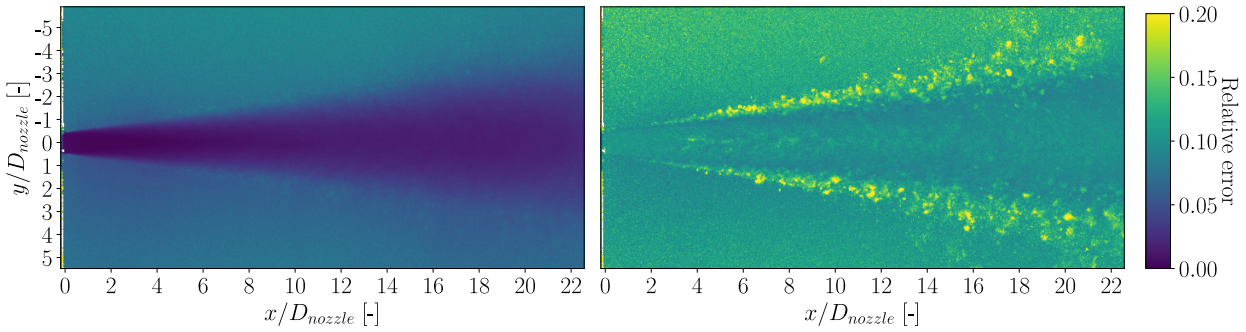

(a) Relative error for mean

(b) Relative error for variance

Figure 3: Error estimation per pixel for 200 samples at an average grayscale value of 1500 for a jet at Re ≈ 62.000 for the mean value (a) and the variance (b) 25 ms after valve opening.

Results

As the visible concentration is highly affected by the chosen average grayscale value, as indicated by figure 2a, the benefits and issues are not consistent within all evaluation factors. Shown in figure 4 three jet snapsshots at the same conditions illustrate the problem. To get a well estimated visible concentration field, see figure 4a, a low average grayscale value is needed. But with the low response the sensor noise is clearly visible along with a sensor artifact visible as vertical lines in the low lit parts of the image. Increasing the seeding concentration to achieve an average grayscale value of 500, see figure 4b, eliminate the sensor artifact at the cost of the concentration estimation due to signal trapping. Only 60% to 70% concentration at the highest value. Sensor noise is also reduced, but can still be seen. If the seeding is further increased so the average grayscale value of 1500, figure 4b, the highest visible concentration decrease to 20% to 30%, but with no visible sensor noise in the areas with high response. Though, as stated in the error analysis, the area from $20D_{nozzle}$ is badly lit with a low concentration, therefore the noise will have a larger effect on the results.

To evaluate the present data quality, unmixedness results from Pitts (1991a,b) are used as benchmark with two important remarks for the comparisons: Jet flows seems to converges towards $\phi_{unmix} \approx 0.23$, but the flow distance to reach this state is strongly dependent on the Reynolds number and the density ratio between jet exit and the environment ($R_\rho = \rho_0/\rho_\infty$). The same tendency is seen for both an increasing R_ρ and Reynolds number, as the flow distance to attain $\phi_{unmix} \approx 0.23$ increase. With this in mind, the present data is expected to fit between the C_3H_8/air data from Pitts (1991a). Further result from Birch et al. (1978) are used to evaluate the centerline concentration decay.

For representing the unmixedness factor and relaxing the response, the data are binned in areas around the center over a length equal to the nozzle radius in x and y in figure 5a. The data shows the difficulties

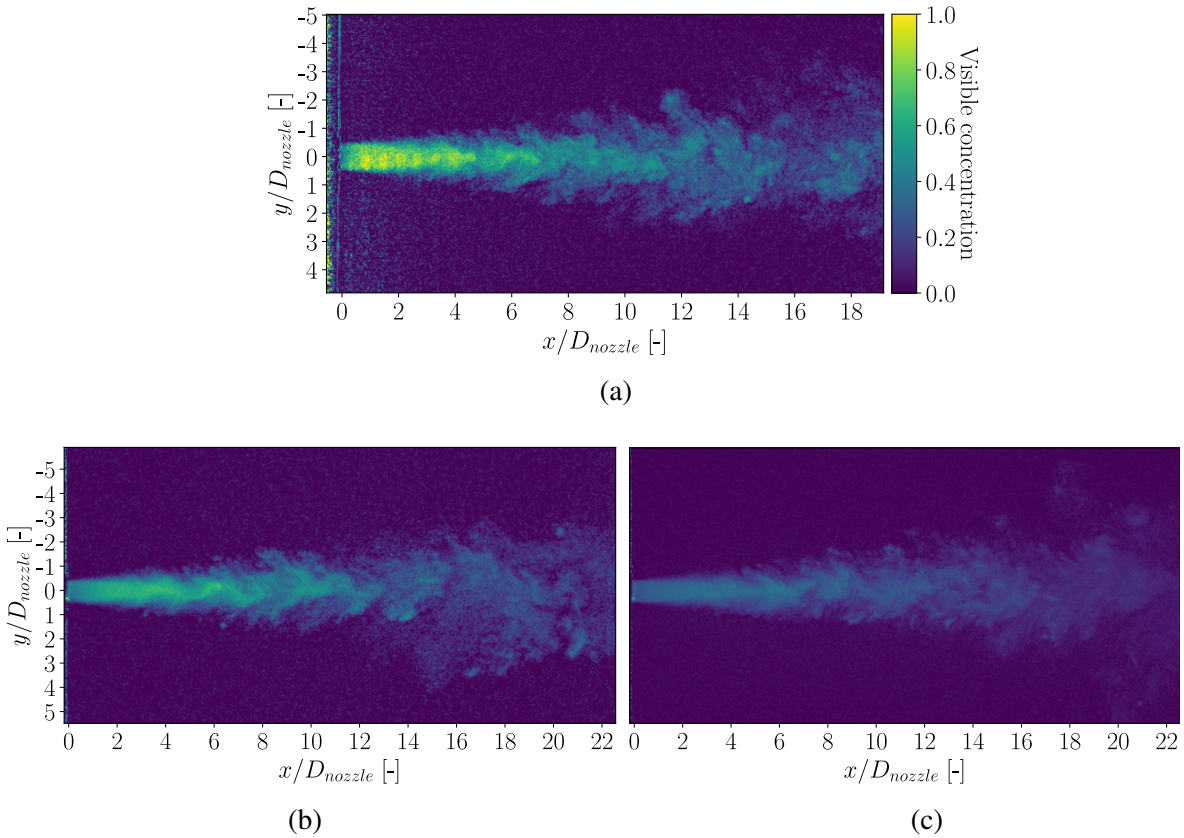

Figure 4: Snapshots of a transient jet 25 ms after valve opening at different average grayscale values. (a) is an average grayscale value of 122, (b) is an average grayscale value of 500, (c) is an average grayscale value of 1500,

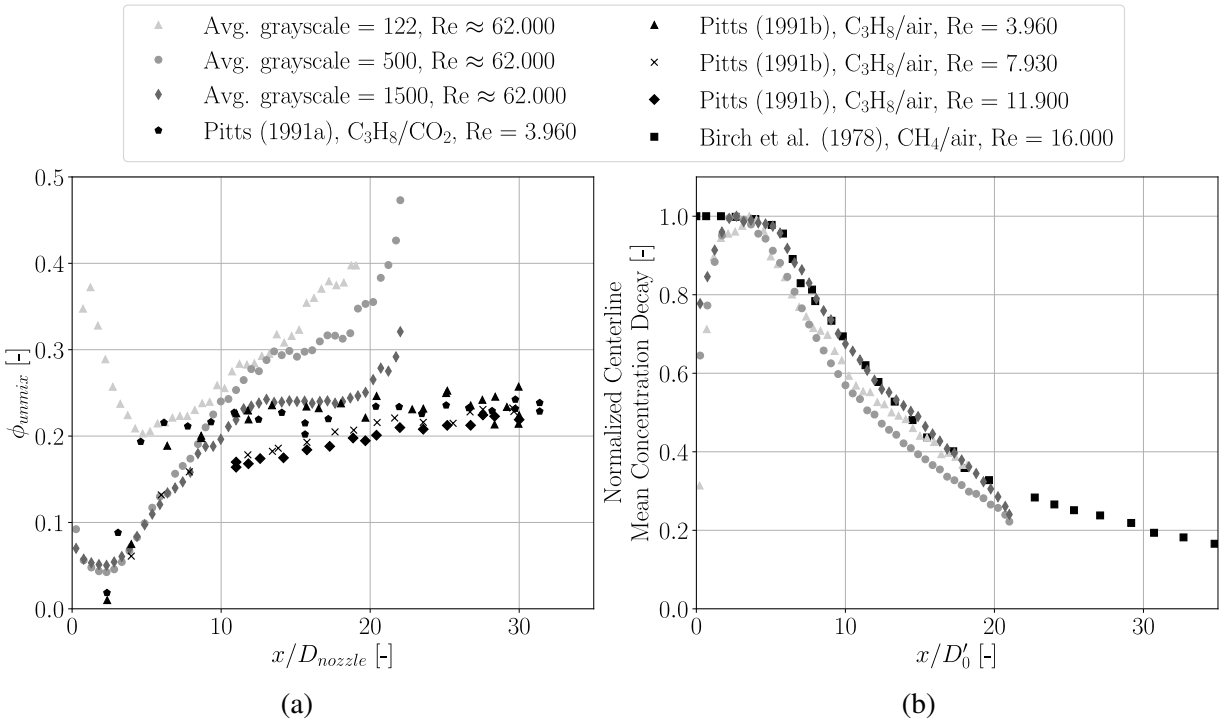

Figure 5: (a) show the unmixedness through the jet centerline against the penetration depth normalized with the nozzle diameter for a jet under no-slip conditions. Compared with data from Pitts (1991a,b). (b) show the normalized centerline concentration decay, normalized with the maximum value measured, plotted against the penetration normalized by length scale incorporating initial turbulence intensity flux information (Papadopoulos and Pitts (1998), $D_0' = 2r_0'$), compared with data from Birch et al. (1978).

with sensor noise when a high concentration estimation is found. Further, a common trait in the data is seen near the jet entrance where a unexpected rise in ϕ_{unmix} appear. For understanding this issue, figure 4 and 2b are studied near the jet entrance. Here a decrease in the concentration, as stated earlier, is seen for all cases. This decrease is due to the visibility and not a results of real concentrations. As the nominator of ϕ_{unmix} builds on the fluctuations of concentration, then if the signal-to-noise ratio (SNR) is too low, the fluctuations are over estimated compared to the average concentration, resulting in a high estimate of ϕ_{unmix}.

By comparison the 122 average grayscale data is not able to predict this parameter due to the low SNR. The 500 average grayscale data show the problem near the jet entrance as stated, but seem to follow the expected trend until $8D_{nozzle}$ where the SNR gets too low. Hereafter the data is comparable to the 122 average grayscale data. For the 1500 average grayscale data it also show the entrance deviance, but fit well with the expected tendency until 18-20D_{nozzle} where the fluctuation gets overestimated compared to the average concentration. The point of this deviation from the comparison fit with the observations from figure 3b. Therefore, the method show with a high signal response, it is able to predict the fluctuations in concentration in most of the near field.

Results of the centerline concentration decay are seen in figure 5b. The figure show the normalized centerline mean concentration decay, normalized with the maximum value measured, and where the streamwise direction is normalised by length scale incorporating initial turbulence intensity flux information $D_0' = 2r_0'$ from Papadopoulos and Pitts (1998). This parameter is a modification to the effective radius were the turbulence intensity flux per unit area is factored in and show to collapse results until the point where the flow reach self-similar state (Dahm and Dimotakis (1990)).

For all datasets the initial low estimation of the visible concentration is again seen, with an erroneous estimation of entrance concentration. But compared to estimation of the centerline unmixedness, the 122 and 500 average grayscale data show a better overall agreement with the tendencies through the flow. The 1500 average grayscale data seem to predict the expected tendency for the concentration decay, but again deviating near the 18-20D_{nozzle} streamwise point.

Conclusion

A high-resolution, high-speed, camera based method on Mie scattering for measuring concentration in a transient jet shooting into a quiescent medium is presented with evaluations on how to define mixing, sample size estimation and some of the challenges with the method. A pixel based two-point linear calibration for each individual shot was used for estimating concentrations. More data were needed to evaluate the precision of the linear response assumption and is set for later studies. Data were presented showing 200 samples provide well statistical estimations of mean concentrations between the shear layer and centerline, while more samples would be advised for statistical estimation of the variance.

With the presented method, it was possible to predict concentration decay and unmixedness tendencies seen in literature for similar jets. Though the data showed challenges providing a realistic estimate on the visible concentration while also predicting the concentration fluctuations due to noise from the camera sensor. To predict the concentration fluctuations, a high sensor response was needed, increasing the signal-to noise ratio (SNR). But as a result of signal trapping the visible concentration was highly reduced.

A decrease in estimated concentration where seen near the jet entrance. It was expected to be an effect from a glare increasing the average grayscale value locally, as the results indicate an increased light response would have this effect.

References

Becker H (1977) Mixing, concentration fluctuations and marker nephelometry. in *Studies in convection : theory, measurement, and applications*. volume 2. pages 45–139. Academic Press

Becker H, Hottel H, and Williams G (1967a) Concentration fluctuations in ducted turbulent jets. *Symposium (International) on Combustion* 11:791–798

Becker HA (1961) *Concentration Fluctuations in Ducted Jet-mixing*. Ph.D. Thesis. Massachusetts Institute of Technology

Becker HA, Hottel HC, and Williams GC (1967b) The nozzle-fluid concentration field of the round, turbulent, free jet. *Journal of Fluid Mechanics* 30:285–303

Becker HA, Hottel HC, and Williams GC (1967c) On the light-scatter technique for the study of turbulence and mixing. *Journal of Fluid Mechanics* 30:259–284

Becker HA and Massaro TA (1968) Vortex evolution in a round jet. *Journal of Fluid Mechanics* 31:435–448

Birch AD, Brown DR, Dodson MG, and Thomas JR (1978) The turbulent concentration field of a methane jet. *Journal of Fluid Mechanics* 88:431–449

Dahm WJA and Dimotakis PE (1987) Measurments of Entrainment and Mixing in Turbulent Jets. *AIAA Journal*

Dahm WJA and Dimotakis PE (1990) Mixing at large Schmidt number in the self-similar far field of turbulent jets. *Journal of Fluid Mechanics* 217:299–330

Dowling DR and Dimotakis PE (1990) Similarity of the concentration field of gas-phase turbulent jets. *Journal of Fluid Mechanics* 218:109

Eberhard S and Munck L (2020) Experimental mixing optimization study with fuel concentrations in air. Bachelor Project. DTU Construct. The Technical University of Denmark

George WK (1990) Governing equations, experiments, and the experimentalist. *Experimental Thermal and Fluid Science* 3:557–566

Hawthorne W, Weddell D, and Hottel H (1948) Mixing and combustion in turbulent gas jets. *Symposium on Combustion and Flame, and Explosion Phenomena* 3:266–288

Hilberg D and Fiedler HE (1994) The application of classical POD and snapshot POD in a turbulent shear layer with periodic structures. *Applied Scientific Research* 53:283–290

Hill PG and Ouellette P (1999) Transient Turbulent Gaseous Fuel Jets for Diesel Engines. *Journal of Fluids Engineering* 121:93–101

Ingvorsen KM, Meyer KE, and Nielsen NF (2011) Planar measurements of velocity and concentration of turbulent mixing in a T-junction. in *Abstract from 9th International Symposium On Particle Image Velocimetry*. Kobe, Japan

Karthick SK, Jagadeesh G, and Reddy KPJ (2016) Visualization of Supersonic Free and Confined Jet using Planar Laser Mie Scattering Technique. *Journal of the Indian Institute of Science* 96

Kukukova A, Aubin J, and Kresta SM (2009) A new definition of mixing and segregation: Three dimensions of a key process variable. *Chemical Engineering Research and Design* 87:633–647

Lam K (2013) Application of POD analysis to concentration field of a jet flow. *Journal of Hydro-environment Research* 7:174–181

Long MB, Webber BF, and Chang RK (1979) Instantaneous two-dimensional concentration measurements in a jet flow by Mie scattering. *Applied Physics Letters* 34:22–24

Lumley J (1967) The Structure of Inhomogeneous Turbulent Flows. *Atmospheric Turbulence and Radio Wave Propagation* pages 166–177

Massalkhi H and Iqbal IS (2022) Measurements of concentration in gas-gas mixing of a jet. Master Thesis. DTU Construct. The Technical University of Denmark

Massey D and Denton N (1988) The Dimensions of Residential Segregation.. *Social Forces* 67:281–315

Papadopoulos G and Pitts WM (1998) Scaling the Near-Field Centerline Mixing Behavior of Axisymlmetric Turbulent Jets. *AIAA Journal* 36

Pitts WM (1991a) Effects of global density ratio on the centerline mixing behavior of axisymmetric turbulent jets. *Experiments in Fluids* 11-11:125–134

Pitts WM (1991b) Reynolds number effects on the mixing behavior of axisymmetric turbulent jets. *Experiments in Fluids* 11-11:135–141

Raffel M, Willert CE, Scarano F, Kähler CJ, Wereley ST, and Kompenhans J (2018) *Particle Image Velocimetry: A Practical Guide*. Springer International Publishing, Cham

Romano G (2002) The effect of boundary conditions by the side of the nozzle of a low Reynolds number jet. *Experiments in Fluids* 33:323–333

Rosensweig RE (1959) *Measurement and Characterization of Turbulent Mixing*. Ph.D. Thesis. Massachusetts Inst. of Tech., Cambridge. Dept. of Chemical Engineering. MIT

Rosensweig RE, Hottel HC, and Williams GC (1961) Smoke-scattered light measurement of turbulent concentration fluctuations. *Chemical Engineering Science* 15:111–129

Sieber M, Paschereit CO, and Oberleithner K (2016) Spectral proper orthogonal decomposition. *Journal of Fluid Mechanics* 792:798–828

Simoens S and Ayrault M (1996) Simultaneous velocity and concentration measurements using Mie scattering and particle image velocimetry in a turbulent air jet. *International seminar on Optical Methods and Data Processing in Heat and Fluid Flow*

Sirovich L (1987) Turbulence and the dynamics of coherent structures Part I: Coherent Structures. *Quarterly of Applied Mathematics* 45:561–571

Tropea C, Yarin A, and Foss J (2007) *Springer Handbook of Experimental Fluid Mechanics*. Springer Berlin Heidelberg

Verzicco R and Orlandi P (1995) Mixedness in the formation of a vortex ring. *Physics of Fluids* 7:1513–1515